JACC: CARDIOVASCULAR IMAGING VOL. 6, NO. 6, 2013

ISSN 1936-878X/$36.00
PUBLISHED BY ELSEVIER INC. http://dx.doi.org/10.1016/j.jcmg.2012.09.020

Myocardial Extracellular Volume Fraction From T1 Measurements in Healthy Volunteers and Mice

Relationship to Aging and Cardiac Dimensions

Tomas G. Neilan, MD,*† Otavio R. Coelho-Filho, MD, MPH,*‡ Ravi V. Shah, MD,*†
Siddique A. Abbasi, MD,* Bobak Heydari, MD,* Eri Watanabe, MD, PhD,§
Yucheng Chen, MD,* Damien Mandry, MD,* Francois Pierre-Mongeon,*‖
Ron Blankstein, MD,* Raymond Y. Kwong, MD, MPH,* Michael Jerosch-Herold, PhD§
Boston, Massachusetts; Campinas, São Paulo, Brazil; and Montreal, Quebec, Canada

OBJECTIVES This study aimed to test the characteristics of the myocardial extracellular volume fraction (ECV) derived from pre- and post-contrast T1 measurements among healthy volunteers.

BACKGROUND Cardiac magnetic resonance (CMR) T1 measurements of myocardium and blood before and after contrast allow quantification of the ECV, a tissue parameter that has been shown to change in proportion to the connective tissue fraction.

METHODS Healthy volunteers underwent standard CMR imaging with administration of gadolinium. T1 measurements were performed with a Look-Locker sequence followed by gradient-echo acquisition. We tested the segmental, interslice, inter-, intra-, and test-retest characteristics of the ECV, as well as the association of the ECV with other variables. Juvenile and aged mice underwent a similar protocol, and cardiac sections were harvested for measurement of fibrosis.

RESULTS In healthy volunteers (N = 32, 56% female; age 21 to 72 years), the ECV averaged 0.28 ± 0.03 (range 0.23 to 0.33). The intraclass coefficients for the intraobserver, interobserver, and test-retest absolute agreements of the ECV were 0.94 (95% confidence interval: 0.84 to 0.98), 0.93 (95% confidence interval: 0.80 to 0.98), and 0.95 (95% confidence interval: 0.52 to 0.99), respectively. In volunteers, the ECV was associated with age ($r = 0.74$, $p < 0.001$), maximal left atrial volume index ($r = 0.67$, $p < 0.001$), and indexed left ventricular mass. There were no differences in the ECV between segments in a slice or between slices. In mice (N = 12), the myocardial ECV ranged from 0.20 to 0.32 and increased with age (0.22 ± 0.02 vs. 0.30 ± 0.02, juvenile vs. aged mice, $p < 0.001$). In mice, the ECV correlated with the extent of myocardial fibrosis ($r = 0.94$, $p < 0.001$).

CONCLUSIONS In healthy volunteers, the myocardial ECV ranges from 0.23 to 0.33, has acceptable test characteristics, and is associated with age, left atrial volume, and left ventricular mass. In mice, the ECV also increases with age and strongly correlates with the extent of myocardial fibrosis. (J Am Coll Cardiol Img 2013;6:672–83) © 2013 by the American College of Cardiology Foundation

From *Noninvasive Cardiovascular Imaging, Cardiovascular Division, Department of Medicine, Brigham and Women's Hospital, Boston, Massachusetts; †Division of Cardiology, Department of Medicine, Massachusetts General Hospital, Boston, Massachusetts; ‡Cardiology Division, School of Medical Science, State University of Campinas (UNICAMP), Campinas, São Paulo, Brazil; §Division of Radiology, Brigham and Women's Hospital, Harvard Medical School, Boston, Massachusetts; and the ‖Division of Noninvasive Cardiology, Department of Medicine, Montreal Heart Institute, Université de Montréal, Montreal, Quebec, Canada. Dr. Neilan is supported by an American Heart Association Fellow to Faculty grant (12FTF12060588) and

The presence of focal myocardial fibrosis is associated with adverse cardiovascular outcomes (1 3). Various imaging techniques have emerged to quantify myocardial fibrosis noninvasively. Cardiac magnetic resonance (CMR) with late gadolinium enhancement (LGE) is the current optimal noninvasive technique for detection and quantification of myocardial scar and replacement fibrosis (4). However, limitations exist to LGE-based techniques for the detection of diffuse or interstitial myocardial fibrosis. Comparison with pathological standards reveals a marked consistent

See page 684

underestimation of both the presence and extent of diffuse fibrosis (5 7). The LGE technique relies on relative enhancement of an abnormal region of myocardium compared with a normal reference. In conditions such as hypertension, sleep apnea, valvular disease, diabetes, obesity, and nonischemic cardiomyopathy, the entire left ventricle may be affected by adverse tissue remodeling, and a normal myocardial reference region may be inappropriately identified. Furthermore, the optimal threshold for quantifying LGE in the presence of diffuse or patchy fibrosis is not well defined (8). These limitations have prompted research into novel CMR-based quantitative techniques for measurement of the myocardial extracellular volume fraction (ECV).

The myocardial ECV increases in proportion to the connective tissue fraction and can be regarded as a continuous measurement of the extent of accumulation of myocardial fibrosis (9 11). T1 mapping is a novel CMR-based technique in which measured differences in R1 (= 1/T1) values before and after gadolinium allow quantification of myocardial ECV (9,12 15). The CMR T1 technique has the potential to differentiate myocardial fibrosis on a continuous scale, from normal myocardium, through diffuse myocardial fibrosis, and ultimately to myocardial scar (16,17). However, limited data exist on the myocardial ECV in a normal healthy population, on the test characteristics of this evolving technique, the optimal CMR protocol for measurement of the myocardial ECV, and on the associations between the ECV and other clinical and imaging variables. Thus, our aims were 2-fold. We first wanted to define a normal reference range in a healthy population, as well as define the test characteristics of the myocardial ECV measurement. The second aim was to test our hypothesis that the myocardial ECV measurement is associated with histological evidence of myocardial fibrosis.

METHODS

Study protocol. The protocol was approved by the Partners Healthcare System Human Subjects Review Committee in the Brigham and Women's Hospital. We recruited healthy volunteer controls by open enrollment. We specifically excluded volunteers with chest pain on exertion; any active or prior history of heart disease, stroke, diabetes, malignancy, sleep apnea, hypertension, an irregular heart rhythm or atrial fibrillation; or any form of kidney disease. Screening consisted of a comprehensive questionnaire detailing medical and medication history, standard anthropometric data, and measurement of blood pressure, pulse, serum creatinine, and hematocrit.

To determine whether aging was associated with a change in the myocardial ECV in mice and to assess whether aging was associated with a change in the extent of myocardial fibrosis, we performed the following protocol in juvenile and aged mice. Juvenile C57BL/6 aged 4 weeks (n = 4) and aged C57BL/6 aged 48 weeks (n = 8) underwent a CMR study. After the CMR study, mice were euthanized, and cardiac sections were analyzed for the presence of myocardial fibrosis using Masson's trichrome. Serum hematocrit was recorded on the day mice were killed immediately after the CMR study. The protocol was approved by the Institutional Animal Care and Use Committee at Harvard University.

Human CMR protocol. All images were acquired with electrocardiographic gating, breath-holding, and the patient in a supine position. Patients were imaged on 3.0-T CMR system (Tim Trio, Siemens, Erlangen, Germany). The basic CMR

ABBREVIATIONS AND ACRONYMS

CI = confidence interval

CMR = cardiac magnetic resonance

ECV = extracellular volume fraction

LGE = late gadolinium enhancement

LV = left ventricular

MOLLI = modified Lock-Locker inversion recovery

ShMOLLI = shortened modified Lock-Locker inversion recovery

previously by an NIH T32 Training Grant (T32HL09430101A1). Dr. Mongeon receives financial support for research from the Montreal Heart Institute Foundation, Montreal, Canada. Dr. Kwong receives salary support from a research grant from the National Institutes of Health (R01HL091157). Dr. Jerosch Herold is supported in part by a research grant from the National Institutes of Health (R01HL090634 01A1); and is listed as co inventor on a pending patent application related to detection of diffuse fibrosis by MRI. All other authors have reported that they have no relationships relevant to the contents of this paper to disclose. Drs. Neilan and Coelho Filho contributed equally to this work.

Manuscript received June 11, 2012; revised manuscript received September 24, 2012, accepted September 26, 2012.

protocol consisted of cine steady-state free-precession imaging (TR, 3.4 ms; TE, 1.2 ms; in-plane spatial resolution, 1.6 × 2 mm) for left ventricular (LV) function and LV mass. Cine imaging was obtained in 8 to 14 matching short-axis (8 mm thick with no gap) and 3 radial long-axis planes. For the calculation of LV mass and function, the endocardial and epicardial borders of the LV myocardium were manually traced on successive short-axis cine images at end-diastole and systole. The papillary muscles were excluded in the LV mass calculation (18), and the LV mass calculation was then indexed to body surface area (19). Left atrial systolic and diastolic volumes were measured using the biplane method as previously described (20). All patients underwent an LGE imaging protocol (TR, 4.8 ms; TE, 1.3 ms; inversion time, 200 to 300 ms) to detect focal myocardial fibrosis. A segmented inversion-recovery pulse sequence for LGE was used starting 10 to 15 min after cumulative 0.15-mmol/kg dose of gadolinium diethylenetriamine pentaacetic acid (Magnevist, Bayer HealthCare Pharmaceuticals Inc., Wayne, New Jersey). LGE images were obtained in 8 to 14 matching short-axis (8 mm thick with no gap) and 3 radial long-axis planes.

Human T1 measurements. T1 measurements were performed with a cine Look-Locker sequence, similar to a standard inversion time scout sequence, with a nonslice-selective adiabatic inversion pulse, followed by segmented gradient-echo acquisition for 17 cardiac phases/times after inversion (TE, 2.5 ms; TR, 5.5 ms; flip angle, 10°; 192 × 128 matrix; 6-mm slice), spread over 2 cardiac cycles (sampling frequency of T1 measurements 100 ms pre-contrast and 55 ms post-contrast, 8-mm slice thickness, TR >3 RR intervals pre-contrast and 2 RR intervals post-contrast) (12,13,21). The Look-Locker sequence was performed in 3 short-axis slices at the level of the basal, mid, and apical left ventricle. Each sequence was repeated in the same LV short-axis slice, once before and 4 to 5 times after the injection of gadolinium spanning a 30-min period (Fig. 1). Specifically, the initial T1 measurement was performed before the administration of gadolinium. The second T1 measurement was performed 3 to 4 min after the initial dose of contrast (0.05 mmol/kg). Immediately after this second T1 measurement, a second dose of contrast was given (0.10 mmol/kg), as LGE imaging was also performed for completeness. The third T1 measurement was performed 3 to 4 min after this second dose of contrast. The final T1 measurement was performed just before the end of the study, an average of 30 to 35 min after the initial dose of contrast. Either 1 or 2 other T1 measurements were performed after the third measurement and before the final measurement at no pre-set intervals.

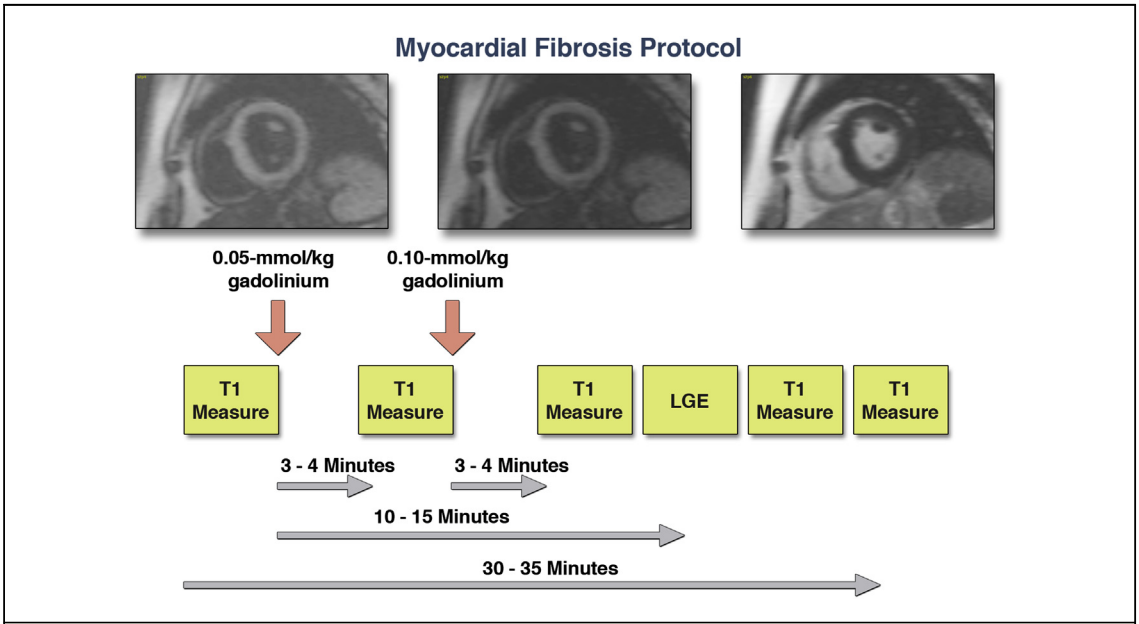

Figure 1. Protocol for Myocardial Fibrosis Imaging

For the myocardial extracellular volume fraction measurement, images were acquired pre contrast and as many as 4 to 5 time points post contrast after a total of 0.15 mmol/kg of gadolinium. Late gadolinium enhancement (LGE) imaging was performed starting 10 to 15 min after administration of gadolinium.

Mouse CMR protocol. Twelve male C57BL/6 mice were imaged on a Bruker 4.7-T CMR imaging platform. For the CMR study, mice were anesthetized with isoflurane (induction 4% to 5%; maintenance 1% to 2% in oxygen from a precision vaporizer). For the CMR study, mice were placed in a special cradle, with electrocardiographic electrodes attached with tape to a front and back paw using electrode gel to optimize contact. For LV volumes and mass, measured after contrast administration, the CMR protocol was built on an electrocardiographically triggered fast gradient-echo FLASH (fast low angle shot) sequence with the following imaging parameters: flip angle, 30°; TR, 8.85 ms; TE, 2.36 ms; matrix, spatial resolution, 0.13 × 0.15 mm. Cine imaging was obtained in 8 to 12 matching short-axis slices (1 mm thick with no gap). LV mass and function were measured in a similar method to the human study. For T1 measurements, we used a Look-Locker sequence with an adiabatic nonslice-selective inversion pulse and the following parameters: flip angle, 15°; TR, 2.2 ms; TE, 1.6 ms; in-plane resolution, 0.13 × 0.15 mm, slice thickness, 1 mm; hyperbolic secant inversion pulse, 6 ms; repetition time per segment, 22 ms; number of averages, 6 (pre-contrast) or 4 (post-contrast). Gadolinium (0.2 mmol/kg) was diluted in saline solution in a 1:10 ratio and administered by multiple intraperitoneal injections in volumes of 200 μl, followed by T1 measurements no earlier than 5 min after each injection. Contrast is rapidly (within <1 min) taken up in the blood and the myocardium after an intraperitoneal injection, and this avoids the difficulty of obtaining tail vein access.

T1 analysis method. For each Look-Locker sequence, the endocardial and epicardial borders of the LV were traced and divided into 6 standard segments, and segments were numbered 1 through 6 starting from the anterior right ventricular insertion point and proceeding in a clockwise direction (Mass Research, Leiden University Medical Center, Leiden, the Netherlands) (Fig. 2). The signal intensity versus time curves for each segment and the

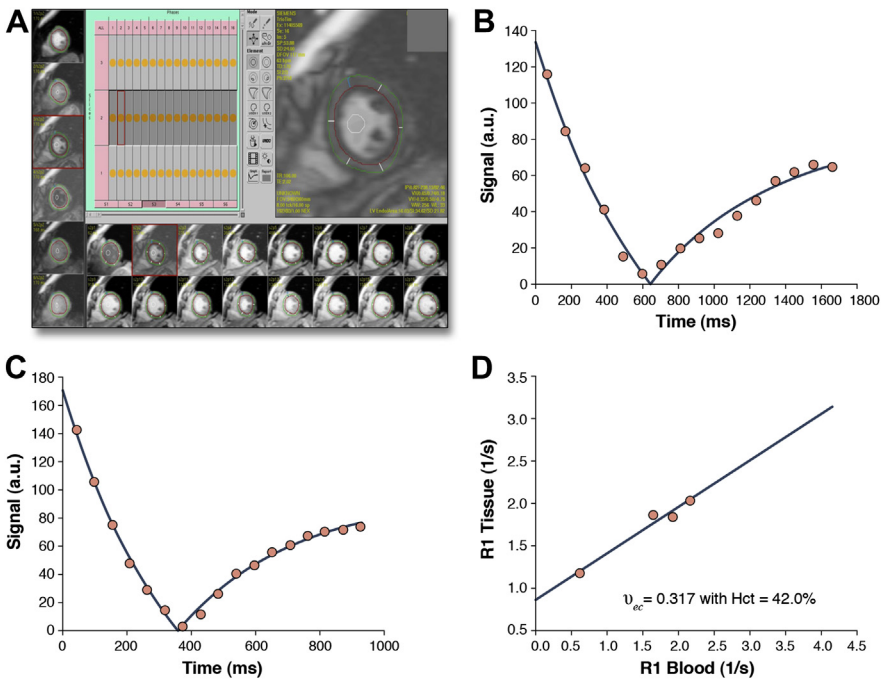

Figure 2. Post-Processing Sequence for Determination of the ECV

For each phase of each slice, the endocardial and epicardial borders of the left ventricle were traced and divided into 6 standard segments. This was repeated for 1 time point pre gadolinium and 4 to 5 time points post gadolinium. A further region of interest was drawn in the left ventricular cavity. **(A)** Segments were then annotated 1 through 6 starting from the anterior right ventricular insertion point and proceeding in a clockwise direction. Representative curves for the inversion time pre **(B)** and post gadolinium **(C)** are shown, displaying shortening of the inversion time. **(D)** The myocardial extracellular volume fraction for this representative healthy volunteer (72 years of age, extracellular volume fraction index of 0.32) is then derived by fitting of the R1 (1/T1) in the myocardium versus the blood and with adjustment for the serum hematocrit (Hct). a.u. = arbitrary units.

blood pool were used to determine segmental T1 through fitting to an analytical expression for the inversion recovery and correction for the radiofrequency pulse alteration of the inversion recovery. The reciprocal of T1 (R1 = 1/T1) was used to plot the myocardial R1 against the R1 in the blood pool. Subsequently, the slope of the association was calculated by linear regression, using measurement points with an R1 <3 s ^{1}. The slope of the linear relationship (the partition coefficient for gadolinium, λ_{Gd}) was based on an extension of the previously used formula:

$$\lambda_{Gd} = \frac{\Delta R_1(tissue)}{\Delta R_1(blood)} = \frac{R_{1t}^{post} \quad R_{1t}^{pre}}{R_{1b}^{post} \quad R_{1b}^{pre}}$$

This formula and the linear model apply to the limit of fast transcytolemmal water exchange, and to meet this condition, only data points with R1 in blood <3.0 s ^{1} were used for the linear regression fits. From the slope of this relationship, the myocardial ECV for all 6 myocardial segments was quantified, as reported previously (12,13), by multiplying each of the segmental λ_{Gd} by (1 − hematocrit in percent/100) (Fig. 2). A global myocardial ECV for each healthy volunteer was then calculated by averaging the 6 myocardial segmental values from the mid-LV short-axis slice.

Mouse blood pressure measurement. Blood pressure was measured in all mice by tail-cuff manometry using a CODA-3 noninvasive blood pressure monitoring system (Kent Scientific, Torrington, Connecticut). The mice were placed in a plastic tube restrainer, occlusion and volume-pressure recording cuffs were placed over their tails, and the mice were allowed to adapt to the restrainer for 30 min before initiating the blood pressure measurement protocol. After the adaptation period, blood pressure was measured for 5 acclimation cycles followed by 10 measurement cycles. Mice were warmed by heating pads during the acclimation cycles to ensure sufficient blood flow to the tail. The animals were monitored closely throughout the measurement protocol, individually heated or cooled as necessary, and removed from the restraint as soon as possible on completing the measurement protocol. All measurements were taken in the afternoon.

Histological analysis. Hearts from all imaged mice were excised and fixed in formalin solution for histological analysis. Short-axis cuts (∼1-mm thickness) of formalin-fixed tissue were processed and embedded in paraffin using standard histological preparations. Mouse myocardial sections were taken of the entire face of a slice, including the septum, LV free wall, and right ventricular wall. The determination of the collagen volume fraction of mice was performed for a mid-level short-axis slice at the same level as the T1 measurement sequences. Sections of ∼5 μm in thickness were stained with Masson's trichrome and viewed under polarized light using a 20× objective. Fifteen to 20 representative areas were chosen in each heart for collagen volume fraction analysis. The Spectrum Analysis algorithm package and ImageScope analysis software (version 9, Aperio Technologies, Inc., Vista, California) were applied to quantify histochemical staining. The fraction of collagen volume is calculated by counting the number of pixels occupied by the stained region and dividing this count by the number of pixels occupied by the entire section.

Statistical analysis. Continuous data are presented as mean ± SD. Continuous data in mice were compared using an independent Student *t* test. Continuous data in humans were compared using analysis of variance and corrected using a Bonferroni correction. We assessed the interobserver and intraobserver variability in a randomly selected group of 16 volunteers. We also aimed to test the repeatability of the ECV measurement when separated by <3 months. We measured the test-retest characteristics in 5 randomly selected volunteers by repeating the measurement of the myocardial ECV within 1 month. Comparison of the interobserver and intraobserver characteristics of the myocardial ECV were made using Bland-Altman plots and determination of the 95% limits of agreement between methods. We determined the intraclass correlation coefficients for the interobserver, intraobserver, and test-retest absolute agreements of the ECV. To test whether the addition of multiple post-contrast measurements of T1 could reduce the variability of the ECV measurement, we compared the variances of the ECV when measured using a single post-contrast T1 and 3 post-contrast T1 values, in combination with a pre-contrast T1 value (for both cases). Comparison of the SDs of ECV from a single post-contrast T1 measurement and the ECV from 3 post-contrast T1 measurements was made using an F-statistic. We also determined the association between the myocardial ECV and other cohort characteristics using a Pearson correlation. We performed a multivariable analysis in humans of the ECV versus age, body surface area, LV mass, and heart rate. The Akaike Information Criterion was used as the criterion for selection of the best prognostic model for a level of significance of 0.05 (22). A 2-sided p value of <0.05 was deemed significant. Regression analysis was

performed in R-statistics software (version 2.9.0, R Foundation, Vienna, Austria); SAS software was used for all other statistical analysis (version 9.1, SAS Institute Inc., Cary, North Carolina).

RESULTS

Baseline parameters in healthy volunteers. Overall, 32 volunteers were recruited, and all were included in the analysis. There were 18 women (56%) and 14 men. The mean age of volunteers was 49 ± 15 years (range 21 to 72 years). The average body mass index was 26 ± 6 kg/m^2, systolic blood pressure was 120 ± 11 mm Hg, diastolic blood pressure was 74 ± 7 mm Hg, heart rate was 68 ± 11 beats/min, and hematocrit was 42 ± 3% (Table 1).

Baseline CMR parameters in healthy volunteers. Baseline CMR parameters are presented in Table 1. In brief, the mean LV end-diastolic volume was 133 ± 29 ml, indexed LV mass was 45 ± 7 g/m^2, right ventricular end-diastolic volume was 131 ± 31 ml, indexed maximal left atrial volume was 33 ± 10 ml/m^2, right ventricular ejection fraction was 53 ± 4%, and LV ejection fraction was 64 ± 7%.

Myocardial ECV in healthy volunteers. LGE was not identified in any normal volunteer. The number of R1 measurements of <3.0 s ^{1} ranged from 3 to 4 (mean, 3.5) in all human studies. We measured the myocardial ECV in 6 segments in 3 slices of the LV (basal, mid-ventricular, and apical). The average myocardial ECV was 0.28 ± 0.03 (range 0.23 to 0.33). There was no difference in the myocardial ECV between basal, mid, or apical slices in healthy controls (0.27 ± 0.02 vs. 0.28 ± 0.03 vs. 0.28 ± 0.03, basal, mid, and apical slices, respectively; p = 0.34 for trend). There was also no difference between segments within a slice; for example, the mid-ventricle was split into 6 segments (0.28 ± 0.04, 0.28 ± 0.04, 0.28 ± 0.04, 0.29 ± 0.04, 0.29 ± 0.03, 0.29 ± 0.03, segments 1 through 6, respectively; p = 0.38 for trend). We measured the interobserver and intraobserver variability in 15 randomly selected studies. The mean interobserver difference was 0.02 ± 0.01 (95% confidence interval [CI]: −0.005 to 0.005) (Fig. 3A), the mean intraobserver difference was 0.01 ± 0.01 (95% CI: −0.005 to 0.005) (Fig. 3B), and the test-retest difference was 0.01 ± 0.01 (95% CI: −0.015 to 0.015). The intraclass coefficients for the intraobserver, interobserver, and the test-retest measurements of the ECV were 0.94 (n = 16, 95% CI: 0.84 to 0.98), 0.93 (n = 16, 95% CI: 0.80 to 0.98), and 0.95 (n = 5, 95% CI: 0.52 to 0.99), respectively. The cohort was separated according to sex. The

Table 1. Patient Characteristics and CMR Variables Grouped by Tertiles of Age Tables

	Cohort (N = 32)	Age <40 Yrs (n = 10)	Age 40–60 Yrs (n = 11)	Age >60 Yrs (n = 11)	p Value
Mean age, yrs	49 ± 15	31 ± 7	51 ± 5	65 ± 5	<0.001
Female	18 (56)	5 (50)	6 (55)	7 (70)	0.23
Body mass index, kg/m^2	26 ± 6	24 ± 4	28 ± 6	27 ± 6	0.27
Systolic blood pressure, mm Hg	120 ± 11	111 ± 11	121 ± 11	125 ± 6	0.31
Diastolic blood pressure, mm Hg	74 ± 7	72 ± 5	72 ± 8	74 ± 5	0.72
Heart rate, beats/min	68 ± 11	63 ± 13	68 ± 8	68 ± 9	0.56
LVEDV, ml	133 ± 24	142 ± 23	141 ± 20	118 ± 27	0.12
LVESV, ml	48 ± 15	50 ± 17	51 ± 9	43 ± 15	0.24
Septal wall thickness, mm	8 ± 1	6 ± 1	7 ± 1	8 ± 1	0.24
Lateral wall thickness, mm	7 ± 1	7 ± 1	7 ± 1	7 ± 1	0.24
LV mass index, g/m^2	45 ± 7	41 ± 9	46 ± 4	47 ± 8	0.23
RVEDV, ml	131 ± 31	154 ± 27	138 ± 24	113 ± 25	0.009
RVESV, ml	61 ± 10	76 ± 8	59 ± 8	55 ± 11	0.015
Indexed maximum LA volume, ml/m^2	33 ± 10	29 ± 9	33 ± 10	37 ± 8	0.12
LVEF, %	64 ± 7	64 ± 9	64 ± 14	63 ± 7	0.66
RVEF, %	53 ± 4	51 ± 5	56 ± 7	51 ± 5	0.53
ECV	0.28 ± 0.03	0.25 ± 0.02	0.27 ± 0.03	0.31 ± 0.02	<0.001

Values are mean ± SD or n (%).
ECV myocardial extracellular volume fraction derived from quantitative T1 measurements; LA left atrial; LV left ventricular; LVEDV left ventricular end-diastolic volume; LVEF left ventricular ejection fraction; LVESV left ventricular end-systolic volume; RVEDV right ventricular end-diastolic volume; RVEF right ventricular ejection fraction; RVESV right ventricular end-systolic volume.

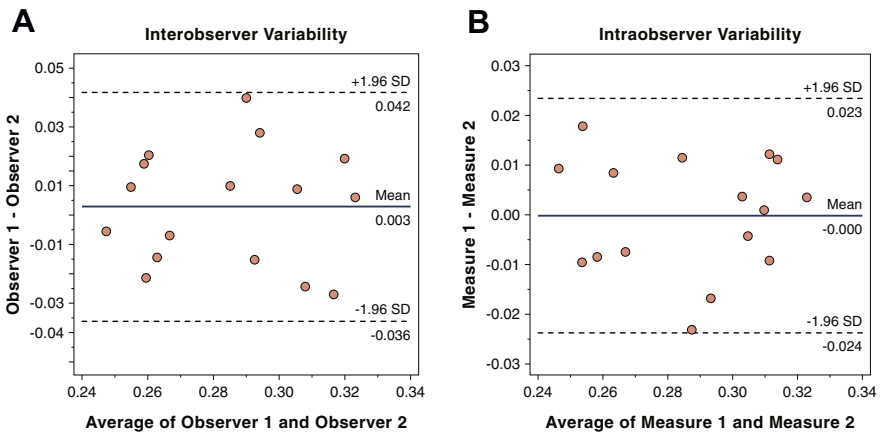

Figure 3. Bland-Altman Plots

The 95% limits of agreement between 2 observers **(A)** and within a single observer **(B)** for 15 randomly selected volunteers is shown.

groups did not differ in age (51 ± 14 years vs. 47 ± 15 years, p = 0.30). There were no difference in the myocardial ECV in males compared with females (0.28 ± 0.03 vs. 0.27 ± 0.03, males vs. females, p = 0.20). To test whether the use of multiple T1 measurements post-contrast reduced measurement variability, we compared the measurement variability of the ECV using a single T1 measurement compared with using 3 post-contrast T1 measurements. We found using a single measurement was associated with a higher SD of 0.041 than using 3 post-contrast T1 measurements, which had as SD of 0.026 (p = 0.02).

Association between the ECV and other variables in healthy volunteers. The myocardial ECV increased with age (r = 0.74, p < 0.001). To test the presence of confounders, we tested the association between pre-contrast blood pool T1 values and heart rate and age. There was no association between the heart rate and the ECV (r = −0.02) and age and pre-contrast blood pool T1 values (r = −0.09). We performed a multivariable analysis for the ECV versus age, body surface area, LV mass, and heart rate. Using this analysis, we got a final multivariable model of the following in which age had the strongest independent association with the ECV (t value = 6.00, p < 0.0001). The entire cohort was split into 3 age ranges of younger than 40, 40 to 60, and older than 60 years of age. There was a graded increase in the myocardial ECV from 0.25 ± 0.02 versus 0.27 ± 0.03 versus 0.31 ± 0.02 with increasing age ranges (p < 0.001) (Fig. 4A). There was no association between the myocardial ECV and heart rate (r = −0.07). There was an association between the myocardial ECV and indexed LV mass (r = 0.52, p < 0.01) (Fig. 4B) and maximal left atrial volume index (r = 0.67, p < 0.001).

Comparison of juvenile and aged mice. As expected, body weight, LV volumes, mass, and stroke volumes were increased in aged mice compared with juvenile mice (Table 2) (23). Both systolic and diastolic blood pressure was unchanged in juvenile compared with aged mice. The myocardial ECV was higher in older compared with younger mice (0.22 ± 0.02 vs. 0.30 ± 0.02, juvenile vs. aged, p < 0.001) (Fig. 5A). Hearts were harvested immediately after the CMR study, and sections were stained using Masson's trichrome. There was an increase in myocardial fibrosis in aged mice compared with juvenile mice (2.1 ± 1.0% vs. 5.8 ± 1.0%, young vs. old mice, p < 0.001). There was a strong association between the myocardial ECV and LV mass (r = 0.81, p < 0.001) and the extent of myocardial fibrosis (r = 0.93, p < 0.001) (Fig. 5B). Representative images are shown from a juvenile and aged mouse (Figs. 5C to 5F).

DISCUSSION

In this study, we measured the myocardial ECV in healthy volunteers and mice using a quantitative T1 technique. The myocardial ECV averaged 0.28 ± 0.03 and ranged from 0.23 to 0.33 in humans. In humans, there was a correlation between myocardial ECV, age, and LV mass. Importantly, there was a consistent increase in the myocardial ECV with increasing age in both volunteers and mice. In mice, we were able to test whether the increase in the myocardial ECV with age was associated with

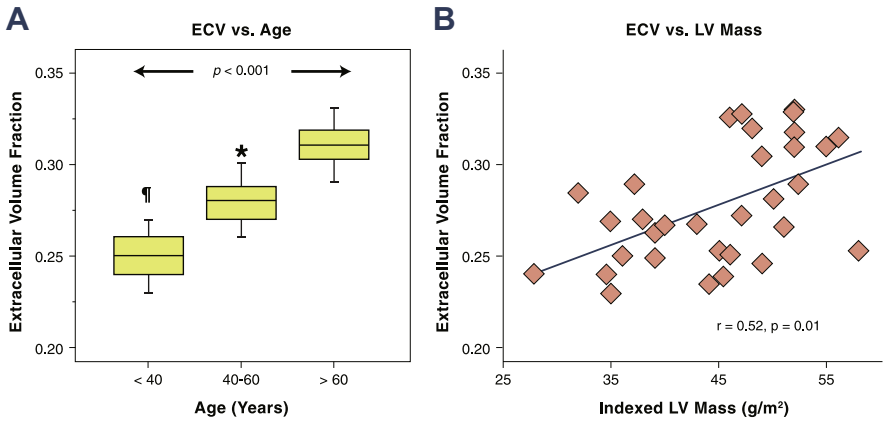

Figure 4. Association Between the Myocardial ECV and Age in Healthy Volunteers

There was a strong association between the myocardial extracellular volume fraction (ECV) and age **(A)** and the myocardial ECVF with indexed left ventricular (LV) mass **(B)**. ¶p < 0.001 vs. age range 40 to 60 years; *p < 0.001 vs. age range >60 years).

expansion of the extracellular matrix. In mice, there was a strong association between the increase in the myocardial ECV and histological evidence of increasing myocardial fibrosis. The range of myocardial ECV in mice was similar to the range observed in our human volunteers. These data suggest that aging is associated with an increase in the myocardial extracellular volume that is detectable using T1 measurements.

These data on noninvasive quantification of the myocardial ECV are both additive to and an extension of previously published work (9,12 15,24 26). Klein et al. (25) used a Look-Locker sequence to calculate a volume of distribution of gadolinium, a myocardial ECVF, in patients with an ischemic cardiomyopathy. They found that the myocardial ECVF was elevated in areas of scar compared to "normal" myocardium. Lee et al. (26) measured myocardial T1 values at 3-T in normal healthy volunteers using a different technique (modified Lock-Locker inversion recovery [MOLLI] technique) and calculated an average ECV of 27%. Some differences exist between the methods used in this and previous studies. First, because we rely on the change of R1 with time, and not on absolute T1 or R1 values, the results are relatively independent of field strength. The technique adjusts for the blood levels of gadolinium by relating the change in R1 in the myocardium and to the corresponding R1 change in blood. Therefore, the estimate of ECV is gadolinium dose independent and largely independent of the clearance of gadolinium from the blood pool, as proven by a previous comparison of the infusion and bolus techniques for ECV quantification (21). The Look-Locker technique used here for T1 imaging allows image acquisition within a single breath-hold per slice, while maintaining a TI resolution of 50 ms for post-contrast measurement acquisition. The protocol used, with at least 3 post-contrast T1 measurements at 3 slice levels, extends a regular CMR study by 5 to 10 min. This method does not depend on the exact timing of the T1 measurement after infusion of gadolinium because multiple measurements of T1 times are recorded repeated multiple times over the course of the CMR study to optimize the accuracy of the partition coefficient determination. A previous

Table 2. Mouse Characteristics and CMR Variables

	Age 4 Weeks (n = 4)	Age 48 Weeks (n = 8)	p Value
Body weight, g	20 ± 1	38 ± 2	<0.001
Heart rate, beats/min	496 ± 41	455 ± 44	0.14
Systolic blood pressure, mm Hg	109 ± 4	114 ± 4	0.08
Diastolic blood pressure, mm Hg	80 ± 4	81 ± 3	0.60
LVEDV, ml	40 ± 9	70 ± 8	<0.001
LVESV, ml	12 ± 5	25 ± 4	<0.001
LV mass, mg	57 ± 4	119 ± 16	<0.001
LVEF, %	70 ± 5	64 ± 6	0.09
Cardiac output, ml/min	14 ± 2	16 ± 4	0.22
Stroke volume, ml	31 ± 9	45 ± 8	0.02
ECV	0.22 ± 0.02	0.30 ± 0.02	<0.001

Values are mean ± SD.
Abbreviations as in Table 1.

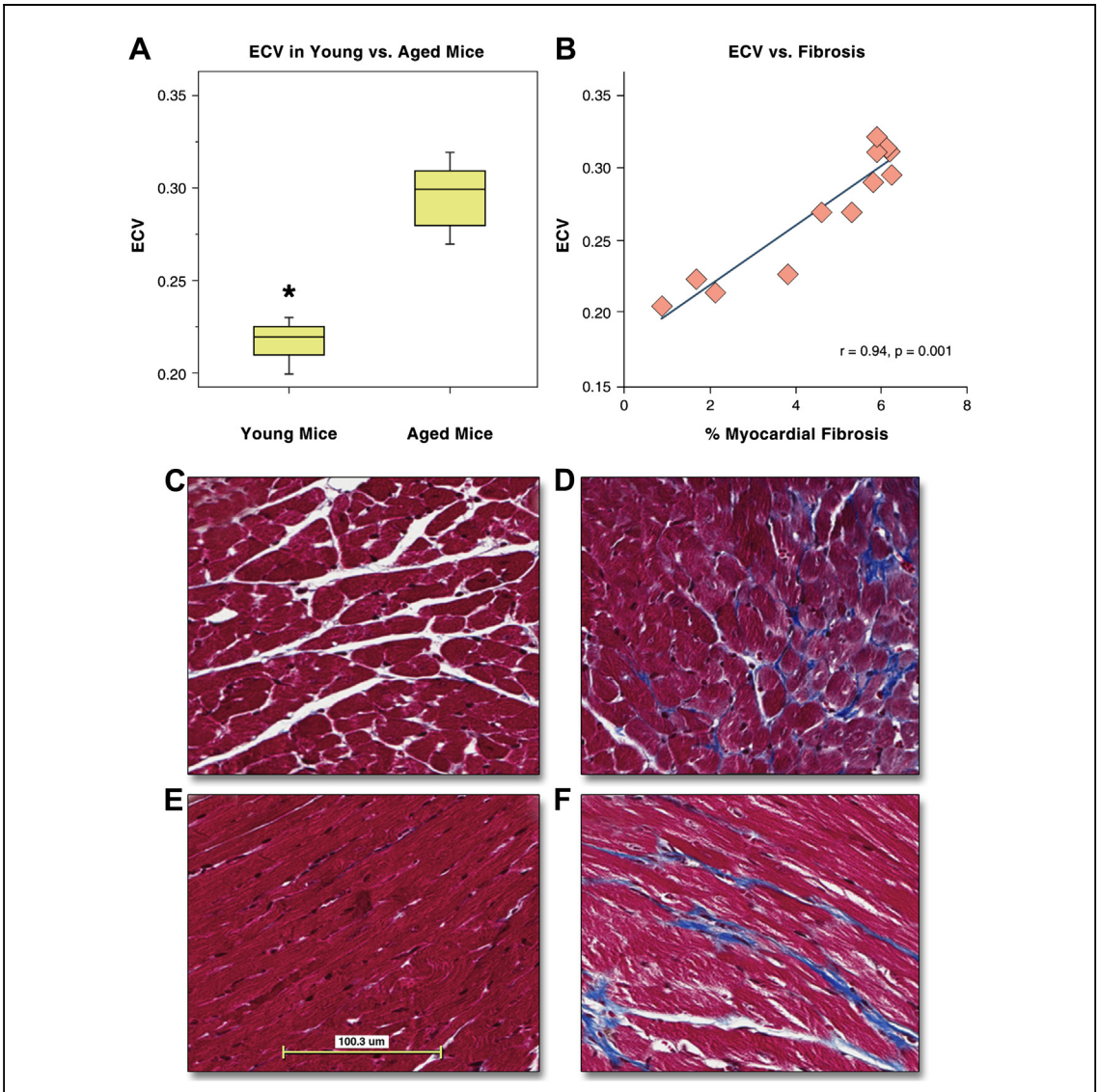

Figure 5. The Myocardial ECV in Juvenile and Aged Mice

Juvenile (4 weeks) and aged (48 weeks) mice underwent a cardiac magnetic resonance (CMR) study. After the CMR study, mice were euthanized, and cardiac sections were harvested for measurement of myocardial fibrosis using Masson's trichrome. **(A)** The myocardial extracellular volume fraction (ECV) was higher in aged mice than juvenile mice (0.22 $\pm$ 0.02 vs. 0.30 $\pm$ 0.02, $p < 0.001$). Histological analysis revealed an increase in the extent of myocardial fibrosis in young versus older mice (2.1 $\pm$ 1.0% vs. 5.8 $\pm$ 1.0%, young vs. old mice, $p < 0.001$). **(B)** There was a strong association between the myocardial ECV and the extent of myocardial fibrosis ($r = 0.93$, $p < 0.001$). Representative images are shown from a juvenile mouse **(C, E)** and an aged mouse **(D, F)** showing normal myocardial architecture stained in **red** with interwoven patches of myocardial fibrosis stained **blue**.

report on the measurement of the partition coefficient for gadolinium contrast in human myocardium (λ_{Gd}), noted a relatively large range for λ_{Gd}, corresponding to a 50% to 60% change in ECV, assuming a constant hematocrit (21). The adjustment of the partition coefficient for gadolinium by multiplication with (1-hematocrit) to determine the myocardial ECV may be 1 reason for the reduced variability in this study (21). Furthermore, >2 T1 measurements were used in combination with a linear regression fit for all values with R1 in blood $<3.0\ s^{-1}$, which reduces variability compared with a 2-point method.

This work has potential clinical and research implications. Aging is associated with a progressive increase in ventricular stiffness and impaired diastolic function (27,28). This age-related impairment of diastolic function is associated with the

development of heart failure and increased mortality (29,30). Similar to published data in patients with known or suspected cardiovascular disease (14), we found that age was associated with an increase in the myocardial ECV in healthy human volunteers in this study. Key differences may relate to the study cohort. We specifically selected healthy subjects free of cardiovascular disease, hypertension, diabetes, and sleep apnea, with a normal blood pressure and a structurally normal heart. However, data are conflicting regarding the relationship between the ECV and age, and the association between the ECV and LV mass (31). We note that in our study there was a significant positive correlation between ECV and LV mass, but in a multivariate regression model for the ECV, there was no significant association between ECV and LV mass, if ECV is simultaneously adjusted by age and sex, suggesting that the association between the ECV and LV mass may be confounded by age. Although limited data exist regarding the association between the ECV and LV mass, there are significant supportive data detailing the strong association between myocardial fibrosis as measured using LGE-based techniques and increased LV mass (32,33). We also show, in wild-type mice, the pathological correlative finding of an increase in myocardial fibrosis. These mice data are consistent with published animal work demonstrating an association between aging and myocardial fibrosis (34,35). Human pathological data are conflicting, but significant supportive data exist suggesting that aging is associated with expansion of the extracellular space and an increase in interstitial fibrosis and appearance of small foci of replacement fibrosis in men and women (36 38). Apoptosis, an enlargement of myocyte size, and extracellular matrix proliferation are other distinctive age-associated changes in myocardial structure. Measurement of the myocardial extracellular volume may provide an early marker of these adverse changes in myocardial tissue structure and may precede overt impairment of ventricular function. To support this, we also found an association between the myocardial ECV and left atrial volume, the latter a commonly used index of diastolic function. However, further work will help determine the natural progression of changes in myocardial structure and function and whether the CMR-detected increase in the myocardial ECV is associated with an increased risk of heart failure.

A robust marker for expansion of the extracellular volume may have extended applicability in cardiovascular monitoring (39). Previous work found a similar normal range for myocardial ECV (14,26) and showed that the ECV can reliably differentiate between normal and abnormal myocardium (14,25). Flett et al. (9) tested whether serial T1 measurements were an index of pathological expansion of the extracellular space. In that study, they found a strong association between the ECV and the extent of myocardial fibrosis in patients with aortic stenosis and hypertrophic cardiomyopathy. Finally, Iles et al. (10) found that post-contrast T1 correlated with histological evidence of myocardial fibrosis in patients with heart failure and extended these finding by showing an association with diastolic function. In contrast, the present study focused on a cohort of volunteers without any history or signs or symptoms of cardiac disease.

Study limitations. This study has to be interpreted within the context of the design format. Image acquisition only extends an average clinical study by 5 min; however, the interpretation currently requires manual tracing of the endocardial contours for 16 to 17 phases from a cine image at as many as 5 time points. We performed a total of 4 to 5 T1 measurements, a pre-gadolinium measurement and 3 to 4 post-gadolinium measurements after a cumulative dose of gadolinium of 0.15 mmol/kg. However, unlike standard clinical practice, the dose of gadolinium was split. Although we acknowledge this as a limitation of the external application, we do not believe that this would likely yield a significant difference in the ECV compared with a single dose of gadolinium. Pathological validation of the CMR-derived ECV as a noninvasive correlate for myocardial collagen content has already been published (19); we did not perform endomyocardial biopsies in our healthy volunteer population or provide serum surrogates for collagen turnover. To attempt to address this limitation, we tested the myocardial ECV in mice and found that, similar to humans, there was an age-related increase in the myocardial ECV. However, important biological differences have been reported regarding the effect of aging in rodents compared with humans that we did not address (40). Other techniques are also available for measuring myocardial T1. These techniques include the MOLLI and the shortened modified Look-Locker inversion recovery (ShMOLLI) methods. Techniques such as MOLLI and ShMOLLI are acquired in the same quiescent window of several cardiac cycles as opposed to data acquisition over the entire cardiac cycle of the Look-Locker cine sequence used in this study. Also, although the acquisition time for the raw data is similar between ShMOLLI and the Look-Locker sequence, the analysis time is faster for either the ShMOLLI or

the MOLLI method (15,41). Data from Kawel et al. (24) using the MOLLI technique with gadolinium diethylenetriamine pentaacetic acid and gadolinium benzyl oxypropionic tetraacetic acid have shown that the relaxivity of the contrast agent may play a role in the ECV determination. It is known that the relaxivity of gadolinium benzyl oxypropionic tetraacetic acid depends on protein concentration, a property that can be potentially a confounding factor in the determination of the extracellular volume fraction. We did not perform echocardiography in healthy controls to determine whether an association existed between measurements of diastolic function and the myocardial ECV. Furthermore, although all controls were free of cardiovascular disease by history, had a normal blood pressure, and had a structurally normal heart on CMR, we did not perform 12-lead electrocardiography to further add to this assessment. However, we did find an association between the myocardial ECV and left atrial volume with an increase in the ECV being associated with larger left atrial volume suggesting a potential link. Multiple pathological processes such as edema and infiltration can expand the extracellular matrix and measurement of the myocardial ECV alone is unable to differentiate between these processes and hence must be interpreted within a clinical context.

CONCLUSIONS

In summary, ECV is a novel and potentially useful index for quantification of the myocardial ECV. In humans, the myocardial ECV increases with age, is associated with LV mass and left atrial volume, and has reliable test characteristics. In mice, the myocardial ECV also increases with age, is also associated with LV mass, and is strongly associated with the extent of myocardial fibrosis. Further work will need to be done to test the application of this technique in patients with cardiovascular disease associated with the development of myocardial fibrosis.

Acknowledgments

The authors thank their CMR technologists for continued excellence.

Reprint requests and correspondence: Dr. Michael Jerosch-Herold, Brigham & Women's Hospital, Harvard Medical School, 75 Francis Street, Boston, Massachusetts 02115. *E mail: mjerosch herold@bics.bwh.harvard.edu.*

REFERENCES

1. Assomull RG, Prasad SK, Lyne J, et al. Cardiovascular magnetic reso nance, fibrosis, and prognosis in dilated cardiomyopathy. J Am Coll Cardiol 2006;48:1977–85.
2. Dweck MR, Joshi S, Murigu T, et al. Midwall fibrosis is an independent predictor of mortality in patients with aortic stenosis. J Am Coll Cardiol 2011;58:1271–9.
3. Kwong RY, Chan AK, Brown KA, et al. Impact of unrecognized myocar dial scar detected by cardiac magnetic resonance imaging on event free sur vival in patients presenting with signs or symptoms of coronary artery disease. Circulation 2006;113:2733–43.
4. Kim RJ, Fieno DS, Parrish TB, et al. Relationship of MRI delayed contrast enhancement to irreversible injury, infarct age, and contractile function. Circulation 1999;100:1992–2002.
5. Azevedo CF, Nigri M, Higuchi ML, et al. Prognostic significance of myo cardial fibrosis quantification by his topathology and magnetic resonance imaging in patients with severe aortic valve disease. J Am Coll Cardiol 2010; 56:278–87.
6. Mewton N, Liu CY, Croisille P, Bluemke D, Lima JA. Assessment of myocardial fibrosis with cardiovascular magnetic resonance. J Am Coll Car diol 2011;57:891–903.
7. Schalla S, Bekkers SC, Dennert R, et al. Replacement and reactive myocardial fibrosis in idiopathic dilated cardiomyopathy: comparison of magnetic resonance imaging with right ventricular biopsy. Eur J Heart Fail 2010;12:227–31.
8. Flett AS, Hasleton J, Cook C, et al. Evaluation of techniques for the quantification of myocardial scar of differing etiology using cardiac mag netic resonance. J Am Coll Cardiol Img 2011;4:150–6.
9. Flett AS, Hayward MP, Ashworth MT, et al. Equilibrium contrast car diovascular magnetic resonance for the measurement of diffuse myocar dial fibrosis: preliminary validation in humans. Circulation 2010;122: 138–44.
10. Iles L, Pfluger H, Phrommintikul A, et al. Evaluation of diffuse myocardial fibrosis in heart failure with cardiac magnetic resonance contrast enhanced T1 mapping. J Am Coll Cardiol 2008; 52:1574–80.
11. Arheden H, Saeed M, Higgins CB, et al. Measurement of the distribution volume of gadopentetate dimeglumine at echo planar MR imaging to quan tify myocardial infarction: comparison with 99mTc DTPA autoradiography in rats. Radiology 1999;211:698–708.
12. Broberg CS, Chugh SS, Conklin C, Sahn DJ, Jerosch Herold M. Quanti fication of diffuse myocardial fibrosis and its association with myocardial dysfunction in congenital heart dis ease. Circ Cardiovasc Imaging 2010;3: 727–34.
13. Jerosch Herold M, Sheridan DC, Kushner JD, et al. Cardiac magnetic resonance imaging of myocardial contrast uptake and blood flow in patients affected with idiopathic or familial dilated cardiomyopathy. Am J Physiol Heart Circ Physiol 2008;295: H1234–42.
14. Ugander M, Oki AJ, Hsu LY, et al. Extracellular volume imaging by magnetic resonance imaging provides insights into overt and sub clinical myocardial pathology. Eur Heart J 2012;54:127–45.
15. Messroghli DR, Radjenovic A, Kozerke S, Higgins DM, Sivananthan MU, Ridgway JP. Modified Look

Locker Inversion recovery (MOLLI) for high-resolution T1 mapping of the heart. Magn Reson Med 2004;52: 141–6.

16. Thornhill RE, Prato FS, Wisenberg G, White JA, Nowell J, Sauer A. Feasibility of the single-bolus strategy for measuring the partition coefficient of Gd-DTPA in patients with myocardial infarction: independence of image delay time and maturity of scar. Magn Reson Med 2006;55:780–9.
17. Thornhill RE, Prato FS, Wisenberg G, Moran GR, Sykes J. Determining the extent to which delayed-enhancement images reflect the partition-coefficient of Gd-DTPA in canine studies of reperfused and unreperfused myocardial infarction. Magn Reson Med 2004;52:1069–79.
18. Rickers C, Wilke NM, Jerosch-Herold M, et al. Utility of cardiac magnetic resonance imaging in the diagnosis of hypertrophic cardiomyopathy. Circulation 2005;112:855–61.
19. Flacke SJ, Fischer SE, Lorenz CH. Measurement of the gadopentetate dimeglumine partition coefficient in human myocardium in vivo: normal distribution and elevation in acute and chronic infarction. Radiology 2001; 218:703–10.
20. Farzaneh-Far A, Ariyarajah V, Shenoy C, et al. Left atrial passive emptying function during dobutamine stress MR imaging is a predictor of cardiac events in patients with suspected myocardial ischemia. J Am Coll Cardiol Img 2011;4:378–88.
21. Schelbert EB, Testa SM, Meier CG, et al. Myocardial extravascular extracellular volume fraction measurement by gadolinium cardiovascular magnetic resonance in humans: slow infusion versus bolus. J Cardiovasc Magn Reson 2011;13:16.
22. Venables W, Ripley B. Modern Applied Statistics with S. 4th edition. New York, NY: Springer, 2002.
23. Wiesmann F, Ruff J, Hiller KH, Rommel E, Haase A, Neubauer S. Developmental changes of cardiac function and mass assessed with MRI in neonatal, juvenile, and adult mice. Am J Physiol Heart Circ Physiol 2000; 278:H652–7.
24. Kawel N, Nacif M, Zavodni A, et al. T1 mapping of the myocardium: Intra-individual assessment of the effect of field strength, cardiac cycle and variation by myocardial region. J Cardiovasc Magn Reson 2012;14:27.
25. Klein C, Nekolla SG, Balbach T, et al. The influence of myocardial blood flow and volume of distribution on late Gd-DTPA kinetics in ischemic heart failure. J Magn Reson Imaging 2004; 20:588–93.
26. Lee JJ, Liu S, Nacif MS, et al. Myocardial T1 and extracellular volume fraction mapping at 3 tesla. J Cardiovasc Magn Reson 2011;13:75.
27. Benjamin EJ, Levy D, Anderson KM, et al. Determinants of Doppler indexes of left ventricular diastolic function in normal subjects (the Framingham Heart Study). Am J Cardiol 1992;70: 508–15.
28. Martos R, Baugh J, Ledwidge M, et al. Diastolic heart failure: evidence of increased myocardial collagen turnover linked to diastolic dysfunction. Circulation 2007;115:888–95.
29. Bursi F, Weston SA, Redfield MM, et al. Systolic and diastolic heart failure in the community. JAMA 2006;296: 2209–16.
30. Redfield MM, Jacobsen SJ, Burnett JC Jr., Mahoney DW, Bailey KR, Rodeheffer RJ. Burden of systolic and diastolic ventricular dysfunction in the community: appreciating the scope of the heart failure epidemic. JAMA 2003;289:194–202.
31. Sado DM, Flett AS, Banypersad SM, et al. Cardiovascular magnetic resonance measurement of myocardial extracellular volume in health and disease. Heart 2012;98:1436–41.
32. Rudolph A, Abdel-Aty H, Bohl S, et al. Noninvasive detection of fibrosis applying contrast-enhanced cardiac magnetic resonance in different forms of left ventricular hypertrophy relation to remodeling. J Am Coll Cardiol 2009;53:284–91.
33. Moon JC, Mogensen J, Elliott PM, et al. Myocardial late gadolinium enhancement cardiovascular magnetic resonance in hypertrophic cardiomyopathy caused by mutations in troponin I. Heart 2005;91:1036–40.
34. Derumeaux G, Ichinose F, Raher MJ, et al. Myocardial alterations in senescent mice and effect of exercise training: a strain rate imaging study. Circ Cardiovasc Imaging 2008;1:227–34.
35. Eghbali M, Eghbali M, Robinson TF, Seifter S, Blumenfeld OO. Collagen accumulation in heart ventricles as a function of growth and aging. Cardiovasc Res 1989;23:723–9.
36. Olivetti G, Melissari M, Capasso JM, Anversa P. Cardiomyopathy of the aging human heart. Myocyte loss and reactive cellular hypertrophy. Circ Res 1991;68:1560–8.
37. Gazoti Debessa CR, Mesiano Maifrino LB, Rodrigues de Souza R. Age related changes of the collagen network of the human heart. Mech Ageing Dev 2001;122:1049–58.
38. Barasch E, Gottdiener JS, Aurigemma G, et al. Association between elevated fibrosis markers and heart failure in the elderly: the Cardiovascular Health Study. Circ Heart Fail 2009;2:303–10.
39. Ho CY, Lopez B, Coelho-Filho OR, et al. Myocardial fibrosis as an early manifestation of hypertrophic cardiomyopathy. N Engl J Med 2010;363: 552–63.
40. Zhang XP, Vatner SF, Shen YT, et al. Increased apoptosis and myocyte enlargement with decreased cardiac mass; distinctive features of the aging male, but not female, monkey heart. J Mol Cell Cardiol 2007;43:487–91.
41. Piechnik SK, Ferreira VM, Dall'Armellina E, et al. Shortened Modified Look-Locker Inversion recovery (ShMOLLI) for clinical myocardial T1-mapping at 1.5 and 3 T within a 9 heartbeat breathhold. J Cardiovasc Magn Reson 2010;12:69.

Key Words: cardiac magnetic resonance ■ extracellular matrix ■ myocardial fibrosis ■ T1 measurements.